DOI: 10.1109/ICTON59386.2023.10207472

Practical Spectral Efficiency Estimation for Optical Networking

Joan M. Gené [(1*)], Jordi Perelló [(1)], Junho Cho [(2)] and Salvatore Spadaro [(1)]

(1) Universitat Politècnica de Catalunya (UPC), Barcelona, Spain.

(2) Infinera Corporation, Holmdel, NJ, USA.

** e-mail: joan.gene@upc.edu*

ABSTRACT

Assigning the right spectral resources is the key to flex-grid optical networking. Finding the optimal spectral allocation is a daunting task, as there are many variables at play that make accurate network models very complex. From a fiber transmission perspective, several impairments, such as amplified spontaneous emission (ASE) noise from amplifiers or nonlinear interreference noise (NLIN) generated through transmission, set a limit on spectral efficiency (SE). From a transceiver perspective, modulation format, signal intensity, and spectral allocation affect the achievable capacity. On top of that, the network conditions are dynamic, causing the channel capacity to change over time. Several models have been proposed to estimate SE, ranging from the simplest to more sophisticated ones. If one is willing to sacrifice a small fraction of accuracy in exchange for a very fast service setup, some bounds can be found to guarantee a static level of service. In this work, we evaluate the degree of inaccuracy introduced by the different strategies and their complexity-accuracy trade-offs.

Keywords: Gaussian Noise model, spectral efficiency, flexible optical networks, modulation formats.

1. INTRODUCTION

Elastic optical networks (EONs) are seen as one of the main enabling technologies in the future backbone networks [1]. A critical task in EONs is to assign the right spectral resources to every connection throughout its lifespan [2]. At the same time, the algorithms must be simple enough if real-time operation is required.

Spectral efficiency (SE) is the way to quantify how many bits per second and per Hertz (b/s/Hz) can be transmitted over a given channel. Estimating SE is in general a complicated task. However, a very simple yet practical case is when the channel is linear with additive white Gaussian noise (AWGN) [3]. In modern uncompensated links with coherent receivers, the optical channel can be assumed to be an AWGN channel. The generation of nonlinear interference noise (NLIN) under a large accumulated chromatic dispersion has been shown to be approximated as an AWGN process, similarly to the generation of amplified spontaneous emission (ASE) introduced by the optical amplifiers. This is the core foundation of the Gaussian noise (GN) model [4].

Under the GN model, the signals, as well as the NLIN and ASE noise, are assumed to be Gaussian. More specifically, the transmitted symbols are assumed to be statistically independent and identically distributed (IID), zero-mean complex circular Gaussian in the time domain even before propagation through fiber, which necessarily means that they are jointly Gaussian in the frequency domain. However, conventional memoryless quadrature amplitude modulation (QAM) symbols are not Gaussian in the time domain, hence only being individually Gaussian in the frequency domain. This invalidates the assumptions of the GN model and compromises its accuracy for QAM signalling.

More sophisticated models have been proposed to overcome such limitation [5]-[8]. They are generally referred to as the enhanced Gaussian noise (EGN) model. Apart from being more precise, it allows to optimize parameters such as the symbol rate [9] to mitigate modulation-dependent NLIN. Contrary to the GN model, the EGN model cannot be modelled with an analytic closed-form expression. It requires tedious numerical computations and Monte-Carlo integrations, making it impractical for a real-time operation. For non-Gaussian signalling, a very simple asymptotic analytical solution has also been derived, which provides good accuracy for mid to long distances [10]. An excellent summary about all models can be found in [11].

From a network operator point of view the question is obvious: which model should be used? In this work, we try to shed light on this complex issue.

2. SPECTRAL EFFICIENCY ESTIMATION

The so-called nonlinear SNR [4] has a linear term coming from the ASE noise generated by the optical amplifiers P_{ase} plus a nonlinear term coming from the Kerr effects occurring when light pulses propagate through optical fibers P_{nli}. The mathematical expression reads

$$SNR = \frac{P_s}{P_{ase} + P_{nli}}, \tag{1}$$

with P_s being the signal power. While P_{ase} is independent of P_s, the nonlinear term is proportional to its 3rd power as $P_{nli} = \eta P_s^3$. In such a case, there is an optimum signal power $P_{opt}^3 = P_{ase}/2\eta$ that maximizes SNR.

In the GN model, the channel's capacity can be estimated using the famous Shannon Formula [3], which in our case reads (2 polarizations)

$$SE_{max} = 2 \cdot log_2 \{1 + SNR_{max}\} = 2 \cdot log_2 \left\{1 + 1/3\left[\eta P_{ase}^2 / 4\right]^{1/3}\right\}. \quad (2)$$

P_{ase} is easily estimated in transparent links as the summation of the independent contributions of all spans. In homogeneous links, all spans contribute equally, and thus the calculation is simplified as

$$P_{ase} = hf \cdot B_o \sum_{i=1}^{N_s} G_i F_i \xrightarrow{\substack{G_i = G \\ F_i = F}} hf \cdot B_o \cdot GF \cdot N_s, \quad (3)$$

where hf is the photon energy (Planck's constant times frequency), B_o denotes the optical bandwidth, G and F are the amplifier's gain and noise figure, respectively, and N_s is the number of spans in the link.

The calculation of the nonlinear coefficient η in Eq. (2) is very much simplified when several assumptions are made [4]. The first one is for the symbols to use ideal Nyquist pulses (rectangular spectrum) and that a matched filter is used at the receiver, which is quite realistic nowadays. The second one is that the span length is over 50 km which is also very common in deployed networks. The third one is link transparency which has also been considered when calculating P_{ase}. Finally, the channel spacing equals the symbol rate and the whole C-band is filled. The last assumption not only makes the calculations simple, but also provides a safety margin for the real case where guard bands are present and some of the channels may eventually be empty. The nonlinear coefficient is then given by

$$\eta_g = \frac{8}{27} \frac{\gamma^2}{\pi |\beta_2|} \frac{1}{R_s^2} \frac{1}{2\alpha} \cdot asinh\left(\frac{1}{2}\pi^2 |\beta_2| B_{wdm}^2 \frac{1}{2\alpha}\right) \cdot N_s. \quad (4)$$

Here, α, β_2, and γ are the fiber's attenuation (m^{-1}), chromatic dispersion ($s^{-2}m^{-1}$), and nonlinear ($W^{-1}m^{-1}$) coefficients, respectively. R_s denotes the symbol rate and B_{wdm} is the whole C-band bandwidth. Notice that like P_{ase}, η is also proportional to the number of spans N_s. This represents the incoherent GN model, where NLIN is assumed to be accumulated incoherently span-by-span [4], which is suitable for optical networks in which interfering channels are added and dropped in a random fashion.

Estimating SE through the GN model is accomplished instantly through closed-form calculations as shown in Eqs. (2)-(4). However, the GN model's accuracy has been shown to be compromised in certain cases [5]-[8]. One big issue is when the signal has a strong non-Gaussianity, which typically happens in two situations: (i) when the transmission distance is too short (only a couple of spans) for the signals to mix over a long period of time due to chromatic dispersion, (ii) when the signal distribution is far from Gaussian and the kurtosis is very small (QPSK is a typical example).

EGN models [5]-[8] have been proposed to reduce the inaccuracy due to the Gaussian assumptions. Although the accuracy improves as more correction terms are added to the GN model, they only provide a numerical solution, not a closed-form solution, and there is generally an accuracy-complexity trade-off. A relatively simple version of the model with fairly good accuracy can be found in [6], which we used in our simulations.

A closed-form correction for the GN model has also been proposed [10] that asymptotically approaches the EGN model as the number of spans increases (very good approximation has been demonstrated after 10 spans of standard fiber and QPSK signals, the modulation for which the GN model is the least accurate). It starts from the ordinary GN model, and determines the modulation-dependent NLIN with improved accuracy by subtracting the degree to which the NLIN is overestimated by the GN model ($\eta = \eta_{gn} - \eta_{corr}$). Under the assumptions running above, the correction term reads

$$\eta_{corr} = \Phi \frac{80}{81} \frac{\gamma^2}{\pi |\beta_2| L_S R_S^2 4\alpha^2} \left(\sum_{n=1}^{N_{ic}} \frac{1}{n}\right) \cdot N_s, \quad (5)$$

where Φ is the kurtosis that equals 1, 17/25, 13/21, and 257/425 for QPSK, 16QAM, 64QAM, and 256QAM, respectively. Φ quickly tends to 3/5 when the QAM order increases. In the case of ideal Gaussian modulation, $\Phi = 0$, so the correction term (5) vanishes and the GN model is perfectly accurate. N_{ic} refers to the number of interfering channels per side.; e.g., $N_{ic} = 2$ means 2 interfering channels on each side of the channel of interest, so a total of 4 interfering channels. The center channel is considered the worst channel (with maximum NLIN).

In this work, we estimate the SE using three options: (i) the plain GN model using Eq. (4), (ii) the asymptotic EGN model using Eq. (5) to improve on Eq. (4), and (iii) the EGN model based on the code provided in [6].

3. RESULTS AND DISCUSSION

We considered a homogeneous link composed of 100 km-spans of standard single-mode fiber (SSMF) with erbium-doped fiber amplifiers (EDFA) to perfectly compensate for span loses (transparency). The simulation parameters are found in the caption of Figure 1. We evaluated 4, 16, 64, and 256-ary QAM with polarization multiplexing (PM). Infinite QAM (∞QAM) and/or ideal Gaussian modulation (GM) are used as a reference.

Figure 1(a) shows the nonlinear parameter η (in dB referenced to W^{-2}) obtained using the EGN model for distances from 100 km to 20,000 km. Notice that the EGN and GN models coincide when GM is used. The asymptotic EGN model is not included for the sake of clarity. The largest reduction of η with respect to the GM is observed at shortest distances where accumulated dispersion is very low. 4QAM has the largest difference (~7.2-dB) while higher order QAMs quickly approach the ∞QAM limit (~3 dB). At 10,000 km, QAM lines become almost parallel to the GM line and the differences are the lowest (~2.5-dB for 4QAM and ~1-dB for ∞QAM, respectively). Figure 1(b) shows the corresponding maximum SNR values, where the differences in SNR (dB) are reduced to 1/3 compared to the differences in η (dB). This is because in Eq. (2), SNR_{max} decreases by 1 dB for every 3 dB increase in η. 4QAM has the best mark (see inset), ~2.4 dB better than the GM at the first span, and the ∞QAM limit is ~1 dB above the GM. After 10,000 km, all SNRs are within a ~0.7 dB difference (see inset).

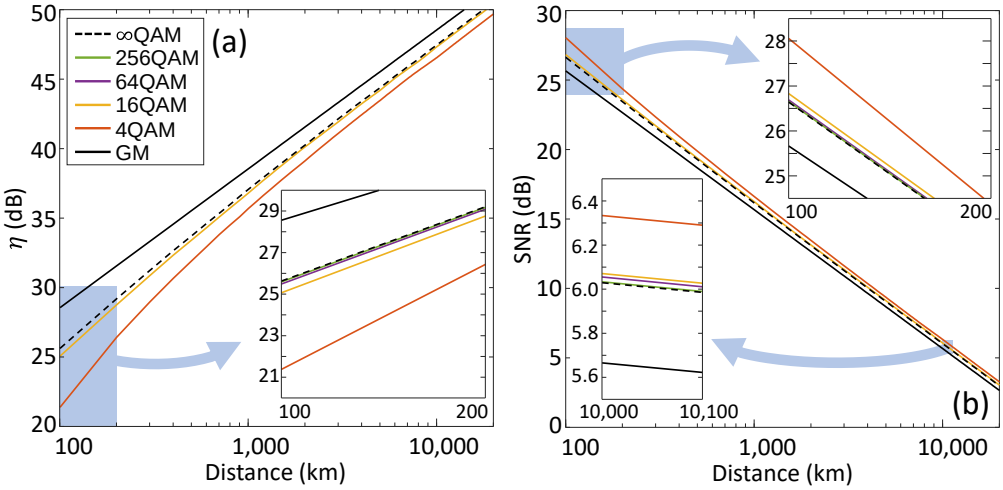

Figure 1. (a) Nonlinear parameter η vs. distance. (b) Maximum SNR vs. distance.

Simulation parameters: $R_s = 50\ GBaud$, $B_{wdm} = 4\ THz$, $\alpha = 0.2\ dB/km$, $D = 17\ ps/(nm \cdot km)$, $\gamma = 1.3\ W/km$, $L_s = 100\ km$, $G = 20\ dB$, $F = 5\ dB$.

Figure 2 shows the maximum SE for all distances and modulation formats obtained by applying Eq. (2) for GM and bit-interleaved coded modulation (BICM) capacity [12] for QAMs, respectively, to the SNR obtained with the GN model (dashed lines) or EGN model (solid lines). A moderate 10% forward-error correction (FEC) code (illustrated by the coloured stripes) has been considered to determine the maximum achievable reach for all finite QAM formats (illustrated by the blue staircase). The reach is upper bounded by the crossing point between each modulation format's SE and the 10% reduction mark. The actual maximum reach is given by the greatest integer multiple of the span length not exceeding this bound (the corresponding span numbers are also indicated in blue). The effect of the discretized spans can be seen in the 256QAM case when the GN model is used. Even though the 10% FEC limit is closer to 200 km than 100 km, rounding down to a full span reduces the reach to 100 km. When the EGN model is used though, the crossing point is just above 200 km which allows reaching the second span. The longer the achievable distance, the less the adverse effect of the discretized spans.

In Figure 2, the maximum theoretical distances (crossing points) are underestimated by 12-20% by the GN model (compare the two distance values for each QAM in the figure). The highest inaccuracy corresponds to the shortest links (100-200 km). The errors of the distance correspond to 1, 1, 3, and 16 spans for 256, 64, 16, and 4-QAM, respectively. For 4-QAM, the error is only valid at distances above 10,000 km, so it is irrelevant for most terrestrial networks where the longest paths rarely exceed 5,000 km. For all QAM formats, the EGN model estimates improved SE by correcting the overestimated NLIN of the GN model. When using the asymptotic EGN model, the underestimation is decreased to 4-10% for all distances (not shown in the figure for the sake of clarity) which correspond to 1, 1, 1, and 5 spans for 256, 64, 16, and 4-QAM, respectively. Because the discrepancies occur only in links with lengths within the coloured vertical bands in the figure, the impact of such inaccuracies on network capacity evaluation is expected to be even less relevant.

Note that in Figure 2, despite the higher SNR of QAMs compared to GM (cf. Figure 1), QAMs achieve a lower SE compared to GM, except for 4QAM at distances above 20,000 km (that are extremely rare in deployed optical links). This is attributed to the shaping gain that GM enjoys over QAM as a linear channel effect.

The GM's SE is approached closely by probabilistic constellation shaping (PCS) that realizes Gaussian probability distributions over QAM symbols and at the same time continuously tunes the SE. It also makes the spectrum allocation more efficient [13]. PCS technology continues to evolve towards mitigating NLIN generation by reducing modulation kurtosis [14], to even exceed the SE of GM shown in Figure 2. Specific PCS implementations and symbol rate optimization enjoy fairly good shaping gains while reducing the NLIN generation [14].

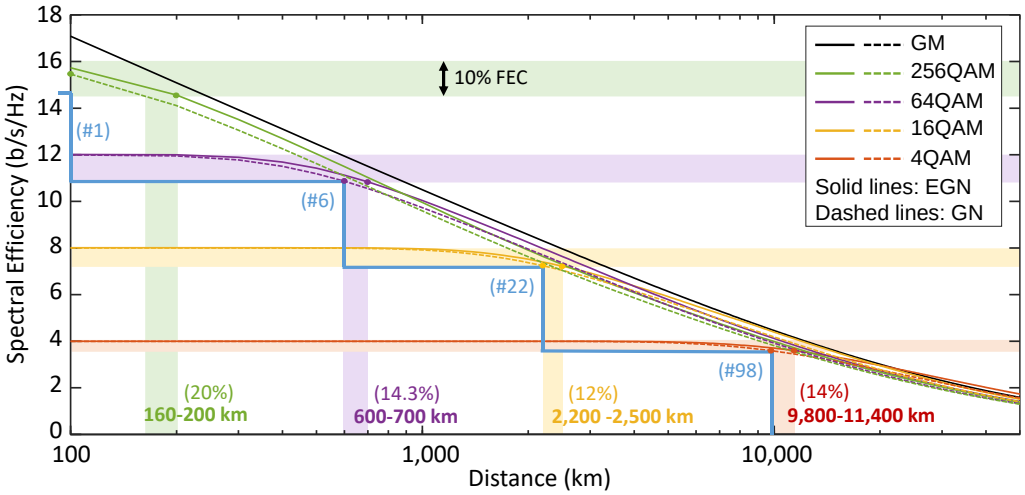

Figure 2. Maximum spectral efficiency vs. distance. (Dashed: GN model, Solid: EGN model)

4. CONCLUSIONS

The plain GN model can be used if a 14-20% underestimation of transmission reach is acceptable on a small percentage of deployed links. Apart from simplicity, the GN model estimation gives a lower bound, providing a moderate safety margin. A fast closed-form analytical correction of the GN model reduces the inaccuracy to 4-10%. The EGN model further improves the accuracy, but the computational load is huge and could be unaffordable when real-time operation is required. On the other hand, if the calculations can be performed offline (SE static precomputation), the EGN could be the way to go.

Several questions remain open. Many worst-case assumptions have been made. How much efficiency is lost in a realistic network? Is the GN model as good as expected when PCS is used? The answers remain for future work.

ACKNOWLEDGEMENTS

This publication is part of the Spanish I+D+i projects TRAINER-A and TRAINER-B (refs. PID2020-118011GB-C21 and PID2020-118011GB-C22), funded by MCIN/AEI/10.13039/501100011033.

REFERENCES

[1] P. J. Winzer and D. T. Neilson, “From Scaling Disparities to Integrated Parallelism: A Decathlon for a Decade,” J. of Lightwave Technology, vol. 35, no. 5, pp. 1099-1115, Mar. 2017.

[2] M. Jinno, et al., “Distance-Adaptive Spectrum Resource Allocation in Spectrum-Sliced Elastic Optical Path Network,” IEEE Commun. Mag., vol. 48, no. 8, pp. 138-145, Aug. 2010.

[3] C. E. Shannon, “A mathematical theory of communication,” The Bell System Technical Journal, vol. 27, no. 3, pp. 379-423, Oct. 1948.

[4] P. Poggiolini, et al., "The GN-Model of Fiber Non-Linear Propagation and its Applications," J. of Lightwave Technology, vol. 32, no. 4, pp. 694-721, Feb., 2014.

[5] R. Dar, et al., "Properties of nonlinear noise in long, dispersion-uncompensated fiber links," Opt. Express 21, 25685-25699 (2013).

[6] R. Dar, et al., "Accumulation of nonlinear interference noise in fiber-optic systems," Opt. Express 22, 14199-14211 (2014).

[7] P. Serena and A. Bononi. "A time-domain extended Gaussian noise model." J. of Lightwave Technology 33, no. 7 (2015): 1459-1472.

[8] A. Carena, et al., "EGN model of non-linear fiber propagation," Opt. Express 22, 16335-16362 (2014).

[9] P. Poggiolini et al., "Analytical and Experimental Results on System Maximum Reach Increase Through Symbol Rate Optimization," J. of Lightwave Technology, vol. 34, no. 8, pp. 1872-1885, April, 2016.

[10] P. Poggiolini, et al., "A Simple and Effective Closed-Form GN Model Correction Formula Accounting for Signal Non-Gaussian Distribution," J. of Lightwave Technology, vol. 33, no. 2, pp. 459-473, Jan., 2015.

[11] A. Bononi, et al., “Fiber Nonlinearity and Optical System Performance”. In: B. Mukherjee, et al.(eds), “Springer Handbook of Optical Networks”. Springer Handbooks (2020).

[12] G. Caire, et al., "Bit-interleaved coded modulation." IEEE T. on Info. Theory 44, no. 3 (1998): 927-946.

[13] J. Perelló, et al., “Evaluation of probabilistic constellation shaping performance in Flex Grid over multicore fiber dynamic optical backbone networks,” J. Opt. Commun. Netw., vol .14, no. 5, pp. B1-B10, May 2022.

[14] J. Cho and R. Tkach, "On the Kurtosis of Modulation Formats for Characterizing the Nonlinear Fiber Propagation," J. of Lightwave Technology, vol. 40, no. 12, pp. 3739-3748, June, 2022.